Separating food intake-dependent and -independent effects in cancer cachexia

Yanshan Liang [1*], Young-Yon Kwon [1*], Sheng Hui [1 2 #]

[1] Department of Molecular Metabolism, Harvard T. H. Chan School of Public Health, Boston, MA, USA

[2] Lead contact

[*] The authors contributed equally

[#] Correspondence: shui@hsph.harvard.edu

Summary

Cancer cachexia is characterized by involuntary weight loss and wasting of fat and muscle tissues, with diminished food intake due to anorexia commonly cited as a cause. However, to what extent reduced food intake drives these symptoms and other cachexia phenotypes, such as fatigue, remains generally unclear in preclinical models and patient populations. Here we demonstrate the critical need to address this question in cancer cachexia research. Using the colon carcinoma 26 (C26) mouse model, we assessed the role of food intake in key cachexia phenotypes. We found that reduced food intake was the predominant driver of body weight loss and wasting of fat and muscle, suggesting no additional causal mechanisms. In contrast, food intake reduction did not affect physical performance, indicating food intake-independent factors in causing fatigue. Thus, depending on the model or patient group, reduced food intake may primarily drive some cachectic phenotypes while having no role in others. Discriminating between food intake-mediated effects and those independent of it is critical for guiding research focus and unraveling the causal pathways of cancer cachexia.

Keywords: cancer cachexia; anorexia; food intake; fat wasting; muscle wasting; fatigue

Introduction

Cancer cachexia is an involuntary wasting condition prevalent in cancer patients, contributing to poor quality of life and reduced survival [1,2]. However, the etiology of the disease remains to be fully understood, and no effective treatment is currently available [3]. One challenge in establishing the causal pathways of cancer cachexia is to distinguish causality from mere association, as evidenced in our previous work showing that the widely assumed cachectic factor IL-6 likely only associates with cancer cachexia [4]. Another often-cited factor contributing to cancer cachexia is reduced food intake due to anorexia [1]. However, to what extent food intake reduction contributes to the body weight loss and also to other phenotypes of cancer cachexia, such as loss of fat mass and muscle mass, impairment of physical performance, and alteration of systemic metabolism, has been rarely rigorously assessed in preclinical models or human patients. This is a critical question because the answer dictates the focus of downstream investigations. For example, food intake reduction is known to cause reduced muscle mass even in healthy animals [5,6]. If reduced food intake alone accounts for most muscle mass loss in cancer cachexia, research should be focused on unraveling mechanisms causing anorexia rather than some active mechanisms of muscle wasting. The same question can be posed for other phenotypes of cancer cachexia, such as adipose tissue wasting and metabolic alterations, both of which are heavily influenced by food intake [7]. Thus, in this study, we focus on the causality of food intake reduction in different cachectic phenotypes and demonstrate the importance of separating food intake-dependent and -independent effects in cancer cachexia research.

Among previous studies of cancer cachexia, a marginal fraction of them controlled for food intake. While the lack of food intake control in patient research is likely due to practical infeasibility, we were only able to find on the order of 10 preclinical studies that used a pair-

feeding strategy (matching daily food intake between cachectic and non-cachectic groups) [8–12] and a couple that employed a caloric restriction strategy (matching total food intake between cachectic and non-cachectic groups) [13,14]. These studies focused on one or two specific phenotypes, such as body weight or adipose tissue wasting, and missed key phenotypes such as physical performance. Thus, a study is needed to systematically delineate the causal roles of food intake reduction in all key phenotypes of cancer cachexia.

Here, we systematically measured how reduced food intake contributes to cachexia phenotypes and metabolic changes in the syngeneic murine colon 26 carcinoma (C26) cancer cachexia model [15] using an isocaloric feeding strategy. Our findings revealed that food intake reduction is a primary driver for body weight loss, fat mass loss, and muscle protein loss in this model, suggesting the lack of additional mechanisms for these cachectic phenotypes. In contrast, food intake reduction does not affect physical performance, highlighting food intake-independent cachectic pathways. Additionally, reduced food intake is responsible for key alterations of systemic metabolism, including reduced circulating glucose and increased ketone body levels, suggesting no need to invoke additional mechanisms to explain these metabolic changes. While these results were obtained for the C26 mode and may well not hold in other models, they clearly demonstrate that distinguishing food intake-induced effects from other cachectic symptoms is crucial for guiding research efforts to identify the causal pathways of cancer cachexia.

Results

Reduced food intake accounts for almost all body weight loss and body composition changes in the C26 model

We first aimed to investigate the contribution of reduced food intake to body weight loss, a primary phenotype of cancer cachexia, in the C26 model. The C26 model was set up by subcutaneously injecting the C26 cells into the syngeneic CD2F1 mice [4,15]. Two weeks post-tumor inoculation, these mice exhibited over 15% body weight loss manifested by fat and lean mass reductions. We refer to this group as the cachectic C26 (cxC26) group. To control for effects due to tumor growth, we included a mouse group using a non-cachectic C26 cell line (ncxC26), which maintained body weight and composition despite similar or bigger tumor size (Figure S1).

The cxC26 mice exhibited a marked reduction in food intake (Figure 1A). Consistent with previous observations [16,17], these mice produced a large amount of masticated food debris (Figure S2). For accurate food intake measurement, mice were single-housed in cages with paper bedding, which allows reliable separation of food debris and bedding materials. To determine the extent to which reduced food intake contributes to body weight loss, we initially employed a standard pair-feeding approach by providing a group of ncxC26 mice with a single portion of food equal to the amount consumed by cxC26 cachectic mice with ad libitum access to food. The pair-fed ncxC26 mice showed similar body weight loss as the cxC26 mice (Figure S1A) under comparable tumor burden (Figure S1C). Fat and lean mass reductions were consistently comparable between the pair-fed ncxC26 and cxC26 mice, suggesting a predominant role for reduced food intake in body weight loss and composition (Figure S1B). A potential caveat in the pair-feeding experiment is that pair-fed mice receive a limited amount of food during the night, which they could consume rapidly. It alters the diurnal food intake patterns, subjecting the animals to a fixed feeding schedule, which can lead to different metabolic and physiological responses distinct from those observed in freely-fed animals [18,19], potentially explaining the

artifact of worse body weight loss in the pair-fed ncxC26 than cxC26 mice (Figure S1A). Thus, to minimize potential differences in feeding behavior between the two groups and to better synchronize their feeding rhythms, we adopted an isocaloric feeding approach in which both ncxC26 and cxC26 mice were provided daily the same amount of food matching the food intake of a group of cxC26 mice ad lib as shown in Figure 1A. Similar to the pair-feeding experiment, the body weight curves were in close match between the isocaloric-fed ncxC26 and cxC26 groups (Figure 1B-C). Furthermore, the extent of both lean mass loss and fat mass loss was also the same between the two isocaloric-fed groups (Figure 1D). Importantly, there was no difference in tumor size between the two groups (Figure 1E). Interestingly, we found that tumor size was smaller in isocaloric-fed ncxC26 mice compared to ad libitum-fed ncxC26 mice, suggesting that reduced food intake slows tumor growth, a phenomenon previously reported in both mouse models [20,21] and human patients [22,23]. These results showed that reduced food intake accounts for almost all of the three key cachectic phenotypes: body weight loss, fat mass loss, and lean mass loss.

Neither energy expenditure nor fecal energy excretion contributes to body weight loss

Our observation that reduced food intake is the sole driver for body weight loss implies a limited role for energy expenditure (EE) in body weight loss, which is often cited to be concomitant with cancer cachexia [24]. To test this, we measured the EE using a metabolic cage system for the isocaloric-fed ncxC26 and cxC26 mice. With identical caloric intake, the time-course EE data in cxC26 mice closely followed that of ncxC26 mice, which was lower than the ncxC26 mice ad lib (Figure 2A). The lack of difference in EE between the two isocaloric-fed groups was also evident in the cumulative EE data (Figure 2B). The metabolic cage data further

showed no difference between the two groups in the respiratory exchange ratio (RER), indicating their similar substrate utilization at the whole-body level (Figure 2C and D).

Another important variable in the energy balance equation is energy excretion, which can be affected by possible malabsorption complications [25] in cancer cachexia. To determine its role in energy balance and body weight loss, we collected all feces produced within the 24 hours before the endpoint from the three groups. We then measured fecal calories using bomb calorimetry. Our results indicated that the two isocaloric-fed groups had similar fecal production, though significantly less than the ncxC26 mice ad lib (Figure 2E). As the fecal energy density was not changed across the groups (Figure 2F), there was reduced but identical total fecal energy excretion in the two isocaloric-fed groups (Figure 2G). Together, these results demonstrated that neither energy expenditure nor fecal energy excretion contributes to body weight loss; instead, reduced food intake accounts for almost all body weight loss as well as body composition in the C26 model.

Reduced food intake is the main driver for muscle protein mass loss in cancer cachexia

Skeletal muscle wasting is a key hallmark of cancer cachexia, and the tumor-secreted factors have been reported to have direct effects on muscle [26,27]. Our body composition data, however, suggested that the muscle wasting could be simply due to food intake reduction. To investigate further the effects of food intake reduction on skeletal muscle mass, at the endpoint, we dissected and weighed the lower limb muscles, including gastrocnemius, soleus, tibialis anterior (TA), and extensor digitorum longus (EDL). Consistent with the lean mass result, reduced food intake for the ncxC26 group resulted in generally reduced muscle mass (comparing the isocaloric-fed ncxC26 group to the ncxC26 ad lib group), albeit to slightly less degree than the cxC26 group in gastrocnemius and soleus (Figure 3A). The muscle mass change was not due

to glycogen mass change because of low muscle glycogen content (<1%) (Figure 3B). As proteins are the main component of muscle tissue, we next assessed the protein content of the gastrocnemius muscle. We observed no significant difference in the protein content of gastrocnemius muscle between isocaloric-fed cxC26 and ncxC26 mice (Figure 3C), indicating a similar magnitude of muscle protein mass loss in the two groups (Figure 3C). This finding was corroborated by the gene expression levels of muscle atrophy biomarkers *Murf1 and Atrogin1* (Figure 3C), which were elevated in the ncxC26 group to the same level as in the cxC26 group. Altogether, these results showed that it is reduced food intake, not some specific cachectic factor, that is the main driver for muscle protein wasting in the C26 model.

Reduced food intake is the primary driver of tissue wasting in mice bearing another cachectic C26 cell line

The finding that reduced food intake alone accounts for body weight loss and tissue wasting is striking. To test the possibility that it is only specific to the cxC26 cell line in our study, we turned to a different cxC26 cell line that originated from the National Cancer Institute (NCI). Mice injected with these cells (referred to as cxC26nci cells) also exhibited reduced food intake (Figure S3A), in line with the anorexia phenotype in the cxC26 mice. Importantly, the non-tumor-bearing pair-fed (NTB pair-fed) mice showed comparable body weight loss and muscle mass reductions to the cxC26nci group (Figure S3B-D), demonstrating that food intake reduction is the primary driver of wasting phenotypes when using this cell line. Note that further recapitulating the cxC26 results is that only the cxC26-nci-bearing mice, but not the NTB pair-fed group, experienced a decrease in grip strength (Figure S3E). Thus, the finding that reduced food intake is the primary driver of body weight loss and tissue wasting is not a peculiar feature of the cxC26 cell line we used.

Physical performance is independent of food intake reduction-induced muscle mass loss in cancer cachexia

To continue assessing the effects of reduced food intake on key phenotypes in cancer cachexia, we next determined its impact on physical performance. For this, we first measured grip strength and found that, surprisingly, compared to the ncxC26 ad lib group, despite reduced muscle mass, the isocaloric-fed ncxC26 group did not show a decrease in grip strength (Figure 3D). In contrast, the isocaloric-fed cxC26 group showed a clear reduction in grip strength (Figure 3D). Grip strength impairment has been reported to be closely associated with fatigue [28]. To subject this finding to further testing, we next measured physical activity, which is well related to fatigue [29] and used for fatigue evaluation [30]. Both daily pedestrian locomotion and daily distance covered in the cage showed increased activity in the isocaloric-fed ncxC26 group, reflecting a foraging behavior under starvation, but not in the isocaloric-fed cxC26 group (Figure 3E). This observation, in line with the grip strength results, suggests that reduced food intake has a limited role in contributing to fatigue. Finally, we performed an additional assay to evaluate fatigue-like behavior [31]. In this test, mice were forced to run on a treadmill until exhaustion to assess their maximal endurance performance. Again, consistent with the grip strength and the physical activity data, the isocaloric-fed cxC26 group showed a substantial reduction in performance while the isocaloric-fed ncxC26 group did not (Figure 3F). Together, these results pointed to a limited role of reduced food intake in contributing to fatigue.

The independence of fatigue on muscle mass is a striking result. A potential caveat for this conclusion is that cachectic animals exhibited slightly but significantly smaller muscle mass compared to their isocaloric-fed non-cachectic counterparts (Figure 3A). Thus, to eliminate this potential caveat and more rigorously test our finding, we subjected a group of ncxC26 mice to a

severe caloric restriction, reducing their food intake by 30% relative to that of the cxC26 mice ad lib starting from day 7 post-tumor injection (Figure 4A). With this approach, the body weight, lean and fat mass, and muscle mass of the caloric-restricted ncxC26 mice were aligned with, and in some cases slightly lower than, those of the cxC26 mice ad lib (Figure 4B-D). We employed the grip strength assay for fatigue evaluation and observed that the grip strength of ncxC26 caloric-restricted mice was comparable to that of the freely fed ncxC26 mice despite substantial food intake reduction (Figure 4E). As the caloric-restricted ncxC26 group now unambiguously had matched muscle mass with the cxC26 group, their largely intact physical performance clearly demonstrated that fatigue is independent of food intake reduction-induced muscle mass loss.

Reduced food intake can account for important metabolic alterations observed in cancer cachexia.

To probe the extent to which reduced food intake contributes to cancer cachexia-associated metabolic changes, we performed a metabolomics analysis on serum samples collected from the ncxC26 ad lib, isocaloric-fed ncxC26, and isocaloric-fed cxC26 mice. Based on principal component analysis (PCA), isocaloric restriction caused significant serum metabolome changes, demonstrated by the distinct separation between the ncxC26 ad lib cluster and the isocaloric-fed ncxC26 cluster (Figure 5A). Note that the isocaloric-fed cxC26 cluster diverged from the isocaloric-fed ncxC26 cluster, suggesting the presence of tumor-dependent metabolic effects. We further identified significantly altered metabolites (adjusted p-values < 0.05) across comparisons with isocaloric-fed cxC26 versus ncxC26 ad lib representing the conventional comparison, isocaloric-fed ncxC26 versus ncxC26 ad lib showing the caloric restriction-induced metabolic changes, and isocaloric-fed cxC26 versus isocaloric-fed ncxC26

showing food intake-independent metabolic changes (Figure S4). As shown in the Venn diagram, 31 out of 54 caloric restriction-induced metabolites overlapped with those identified in the conventional comparison (Figure 5B), suggesting that metabolomics results on cancer cachexia can be misleading in terms of reflecting metabolic abnormalities if food intake is not controlled for. Only 26 out of 72 significantly altered metabolites from the conventional comparison dataset overlapped with net cancer cachexia-associated metabolic changes. Changes in important metabolic indicators such as glucose and ketone bodies (acetoacetate and 3-hydroxybutyrate) (Figure 5C) and liver glycogen content (Figure 5D) are likely consequences of reduced food intake instead of reflecting metabolic abnormalities in cancer cachexia. All the cancer cachexia-associated significant metabolites are listed in Table S1. To further investigate the biological significance of these changes, we performed pathway enrichment analysis on the altered metabolites (Figure S5). This analysis shows significant enrichment in energy metabolic pathways such as the citric acid cycle, gluconeogenesis, carnitine synthesis, the mitochondrial electron transport chain, glycolysis, and the malate-aspartate shuttle. These findings suggest that despite similar overall energy balance between the two groups there is reprogramming of energy metabolism in cancer cachexia. How cachectic tumor induce these changes and whether they contribute to food intake-independent cachectic phenotypes such as fatigue are important topics for future studies.

Discussion

This study demonstrates the importance of separating food intake-dependent and -independent effects in cancer cachexia research. The findings that key cachectic phenotypes, including body weight loss, mass loss of adipose tissue and muscle, and alterations of key metabolites, are mostly attributable to reduced food intake in the C26 model inform that a search

for new mechanisms for these phenotypes may not be justified in this model. Instead, the finding that fatigue occurs independently of reduced food intake highlights novel mechanisms that warrant further investigation. The extent to which reduced food intake contributes to cachectic phenotypes is generally different in different preclinical models and different subtypes of patients. Thus, we propose to make it a standard procedure to get accurate food intake data and perform rigorous control for food intake in studies of cancer cachexia.

Accurate food intake measurement is not as straightforward as it may sound. This is evidenced in contradicting results in the literature on the C26 model, with reduced food intake measured in some studies [32–34] and no change in food intake reported in others [35–37]. While it is a possibility that cachectic C26 cell lines from different laboratories are fundamentally different, it is more conceivable that the discrepancy arose from the technical challenges of food intake measurement. As shown in Figure S2, cachectic mice tend to make large quantities of masticated food debris. The food debris further resembles common cage bedding materials in color, size, and shape, making them difficult to be separated. Thus, without a careful account of the food debris, food intake measurement can be incorrect.

Our results caution against using the expression of the genes *Murf1* and *Atrogin1* as markers of muscle atrophy in cancer cachexia. Consistent with the muscle mass data, food intake reduction alone induces their expression to the same level as in the cachectic C26 mice. Thus, while these gene markers may reflect muscle mass loss, their use as an indication of reduced food intake-independent, active muscle wasting is not validated.

It was surprising to find that the loss of adipose tissue and muscle mass was simply due to the food intake reduction in the C26 model. This is because the model has often been used for studying active mechanisms of adipose tissue wasting [12,36] and muscle wasting [38,39]. These

studies generally did not check food intake or conduct food intake control, and thus cannot distinguish whether the wasting was primarily due to food intake reduction or some active mechanisms. While we cannot rule out the complete lack of additional mechanisms of tissue wasting, our results indicate a minor role for them in this model.

Our study showed no elevation of total energy expenditure in the C26 model. Despite being commonly cited as a contributor to body weight loss in cancer cachexia, energy expenditure elevation has only been observed in limited number of cases, including some patients with lung and pancreatic cancer [40], as well as preclinical models such as Lewis lung cancer (LLC) cachexia model [24] and a skin cancer cachexia model [41]. Significantly lower physical activity was observed in cxC26 mice, suggesting that energy may be redirected toward other biological processes. To assess the impact on energy balance, activity-related energy expenditure at day 12 post-tumor inoculation was estimated using a mass-specific energy cost per unit of physical activity, averaging 60 cal/km/g body weight [42] (Figure S6). Although there was a trend toward decreased activity-related energy expenditure, the difference amounted to a few percent of TEE, which did not result in a measurable change in total energy expenditure. We however cannot rule out the possibility of elevated energy cost arising from biological processes such as an active immune response in cachectic mice, though the increase would likely be relatively small and difficult to detect in metabolic cage measurement.

Our results revealed that fatigue does not necessarily depend on food intake reduction or muscle mass loss in cancer cachexia. With comparable muscle loss induced by reduced food intake, only the cachectic animals exhibited reductions in grip strength, physical activities, and maximum exercise capacity, while non-cachectic animals remained as competent as the ad lib control. In line with our results, a study using a lung cancer cachexia model compared caloric-

restricted mice with cachectic mice and observed similar reductions in fat mass, lean mass, and skeletal muscle mass, but no change of muscle function in the caloric-restricted group [43]. Grip strength has been reported to be preserved [44], and exercise endurance has been shown to increase [45] in humans after caloric restriction, which aligns with what we found in the calorie-restricted non-cachectic mice. Thus, different from muscle wasting or muscle atrophy, fatigue is a distinct phenotype in cancer cachexia. Fatigue could be due to either muscle function impairment [46] or neural dysfunction [47], which so far has been understudied in cancer cachexia research and deserves more attention in the field.

By isolating out the effects of reduced food intake, the goal is to simplify the complex problem of cancer cachexia and ultimately establish the causal pathways of cancer cachexia. We do not downplay the role of reduced food intake or anorexia in cancer cachexia. Instead, as shown in our results, reduced food intake plays a dominant role in multiple phenotypes of cachexia. We simply argue for separate treatments of food intake-dependent and -independent phenotypes while searching for the underlying mechanisms (Figure 5E). In this structure of a causal pathway, a successful strategy for therapeutic development might be to act separately on appetite and physical performance. In line with our view, several clinical trials targeting the ghrelin pathway for increased food intake had no effects on hand grip strength and overall survival despite reported improvements in lean body mass [48,49]. While inhibition of GDF15 signaling was reported to have mitigated not only body weight loss but also physical performance impairment through rescuing appetite in preclinical cancer cachexia models (HT-1080 [50] and TOV21G (ovarian cancer) [51]), the mechanism by which GDF15 impacts physical performance is unclear and the physical performance in a recent clinical trial of an anti-GDF15

antibody had inconsistent dose-dependence [52]. Thus, a future effective treatment is likely a combination of two drugs, targeting reduced food intake and fatigue.

Limitations of the study

Our study has several limitations. First, the cachectic phenotypes we focused on do not cover important ones such as systemic inflammation [53], malabsorption [54], altered gut microbiota [55], and liver function [56] which can contribute to the overall condition of the disease. Second, while our overall conclusion that food intake reduction alone can explain some key cachectic phenotypes still holds regardless results from a different model, our experiments were carried out on one cancer cachexia model and thus the conclusions regarding the extent of the effects of food intake on specific phenotypes may not be generalized to other models. Third, we focused on male mice. It is of great interest to measure the effects of food intake in female cachectic mice in future studies.

Resource availability

Lead contact

Further information and requests for resources and reagents should be directed to and will be fulfilled by the lead contact, Sheng Hui (shui@hsph.harvard.edu).

Materials availability

This study did not generate new unique reagents.

Data and code availability

- Source data supporting the findings of this study are accessible from Mendeley Data with doi: 10.17632/smfbybvgfm.1.
- This paper does not report original code.
- MS raw files are accessible from Metabolomics Workbench Repository with project ID ST004321.
- Any additional information required to reanalyze the data reported in this paper is available from the lead contact upon request.

Acknowledgements

We would like to thank Dr. Andrea Bonetto (cxC26) and Dr. Nicole Beauchemin (ncxC26) for graciously providing the cell lines used for our studies. We are grateful to Dr. Tobias Janowitz, Dr. Eileen White, and Dr. Marcus Goncalves for their critical reading and valuable suggestions of the manuscript. We thank Karen E. Inouye for the technical support with the metabolic cages and EchoMRI, and Guangru Jiang for the help in fecal energy excretion measurement. This work was delivered as part of the CANCAN team supported by the Cancer Grand Challenges partnership funded by Cancer Research UK (CGCATF-2021/100034) and the National Cancer Institute (OT2CA278654).

Author contributions

Y.L., Y.K., and S.H. conceived the experiments and wrote the manuscript. Y.L. and Y.K. performed the experiments and analyzed the data. S.H. secured funding. All the authors reviewed the results and approved the final manuscript.

Disclosure and competing interests statement

The authors declare no competing interests.

Figure titles and legends

Figure 1. Reduced food intake is the main driver of body weight loss and body composition changes.

CD2F1 male mice were inoculated with 1×10^6 ncxC26 or cxC26 cells subcutaneously. **(A)** Food intake of ncxC26 and cxC26 mice ad lib. **(B)** Percentage change in body weight, **(C)** absolute initial and endpoint body weight, (**D**) body composition measured using EchoMRI at the endpoint, and **(E)** tumor size at the endpoint, for ncxC26 ad lib, isocaloric-fed ncxC26, and isocaloric-fed cxC26 groups. **(A)** n=16 for ncxC26 ad lib and n=16 for cxC26 ad lib. **(B)** n=20 for ncxC26 ad lib, n=20 for isocaloric-fed ncxC26, n=15 for isocaloric-fed cxC26. **(C-D)** n=18 for ncxC26 ad lib, n=18 for isocaloric-fed ncxC26, n=14 for isocaloric-fed cxC26. **(E)** n=21 for ncxC26 ad lib, n=22 for isocaloric-fed ncxC26, n=22 for isocaloric-fed cxC26. All data are shown as the mean ± s.d. Significance of the differences **(C-E)**: ns not significant, *P < 0.05, **P < 0.01, ***P < 0.001, **** P<0.0001 between groups by one-way ANOVA followed by Tukey post hoc comparison.

Figure 2. Neither energy expenditure nor energy excretion contributes to body weight loss.

(A) Hourly energy expenditure from day 6 to day 12 post-inoculation. **(B)** Cumulative energy expenditure during full day, daytime, and nighttime. **(C)** Hourly respiratory exchange ratio from day 6 to day 12 post-inoculation. **(D)** Average respiratory exchange ratio. **(E)** Fecal production within 24 hours before euthanasia. **(F)** Fecal energy density. **(G)** Total fecal energy excretion

within 24 hours before euthanasia. **(A-D)** n=4 per group. **(E-G)** n=8 for ncxC26 ad lib, n=8 for isocaloric-fed ncxC26, and n=5 for isocaloric-fed cxC26. All data are shown as the mean ± s.d. Significance of the differences **(B, D, E-G)**: ns not significant, *P < 0.05, **P < 0.01, ***P < 0.001, **** P < 0.0001 between groups by one-way ANOVA followed by Tukey post hoc comparison.

Figure 3. Reduced food intake induces muscle protein wasting but not fatigue in cancer cachexia.

(A) Muscle mass. **(B)** Muscle glycogen content. **(C)** Muscle protein content, total protein mass in gastrocnemius calculated by multiplying the averaged protein content with muscle mass, and mRNA expression levels of atrophy markers in the gastrocnemius. **(D)** Grip strength. **(E)** Changes in daily pedestrian locomotion and distance in cages comparing day 12 to the average during days 0-5. **(F)** Maximum exercise capacity (running on a treadmill until exhaustion). **(A)** n=23 for ncxC26 ad lib, n=24 for isocaloric-fed ncxC26, n=28 for isocaloric-fed cxC26. **(B)** n=6 for ncxC26 ad lib, n=7 for isocaloric-fed ncxC26, n=6 for isocaloric-fed cxC26. **(C)** n=10 for ncxC26 ad lib, n=12 for isocaloric-fed ncxC26, n=8 for isocaloric-fed cxC26 in the protein content measurement; n=23 for ncxC26 ad lib, n=24 for isocaloric-fed ncxC26, n=28 for isocaloric-fed cxC26 in the protein mass calculation; n=10 for ncxC26 ad lib, n=12 for isocaloric-fed ncxC26, n=9 for isocaloric-fed cxC26 in the muscle gene expression measurement. **(D)** n=22 for ncxC26 ad lib, n=23 for isocaloric-fed ncxC26, n=23 for isocaloric-fed cxC26. **(E)** n=4 for ncxC26 ad lib, n=4 for isocaloric-fed ncxC26, n=6 for isocaloric-fed cxC26. **(F)** n=6 for ncxC26 ad lib, n=8 for isocaloric-fed ncxC26, n=7 for isocaloric-fed cxC26. All data are shown as the mean ± s.d. Significance of the differences in all figures: ns not significant, *P < 0.05, **P

< 0.01, ***P < 0.001, **** P < 0.0001 between groups by one-way ANOVA followed by Tukey post hoc comparison.

Figure 4. Fatigue is independent of food intake reduction-induced muscle mass loss in cancer cachexia.

A group of ncxC26 mice was under severe caloric restriction (severeCR), receiving 30% less food intake than a group of cxC26 mice ad lib starting from day 7 post-tumor inoculation. **(A)** Food intake. **(B)** Percentage change in body weight. **(C)** Percentage change of body composition **(D)** Muscle mass. **(E)** Grip strength at the endpoint. **(A-E)** n=6 for ncxC26 ad lib, n=6 for ncxC26 severeCR, and n=5 for cxC26 ad lib. **(B-E)** are shown as the mean ± s.d. Significance of the differences **(C-E)**: ns not significant, *P < 0.05, **P < 0.01, ***P < 0.001, **** P < 0.0001 between groups by one-way ANOVA followed by Tukey post hoc comparison.

Figure 5. Reduced food intake accounts for important metabolic alterations observed in cancer cachexia.

(A) Principal component analysis of the serum metabolomics. **(B)** Venn diagram of the significant metabolites found in different comparisons. Metabolites with adjusted p-values < 0.05 by one-way ANOVA followed by Tukey post hoc comparison were considered as significant changes. **(C)** Serum glucose and ketone bodies, acetoacetate, and 3-hydroxybutyrate. **(D)** Liver glycogen content. **(E)** Diagram summarizing the food intake-dependent and -independent cachectic phenotypes in the C26 model. **(A-C)** n=11 for ncxC26 ad lib, n=10 for isocaloric-fed ncxC26, n=12 for isocaloric-fed cxC26. **(D)** n=6 for ncxC26 ad lib, n=7 for isocaloric-fed ncxC26, n=6 for isocaloric-fed cxC26. **(C and D)** are shown as the mean ± s.d. Significance of

the differences **(C and D)**: ns not significant, *P < 0.05, **P < 0.01, ***P < 0.001, **** P < 0.0001 between groups by one-way ANOVA followed by Tukey post hoc comparison.

STAR METHODS

KEY RESOURCES TABLE

EXPERIMENTAL MODEL AND STUDY PARTICIPANT DETAILS

Cell culture

The cachectic C26 (cxC26) and non-cachectic (ncxC26) cells were kind gifts from Andrea Bonetto [15] and Nicole Beauchemin, respectively. Nicole Beauchemin obtained the ncxC26 cells from Brattain MG, who established the C26 (also named CT26 or colon carcinoma 26) cell line [57]. The C26nci (C26 from the National Cancer Institute) was a kind gift from Robert Jackman [58]. All the cell lines were maintained in high-glucose DMEM (Corning) with 10% fetal bovine serum (FBS, R&D Systems) and 1% penicillin/streptomycin (P/S, Hyclone) at 37 °C and 5% CO_2. Prior to tumor injection, cells were cultured and used at passages 4 to 6 to ensure consistency and minimize variability associated with extended passaging.

Animals

To describe animal experiments, we have taken into account the recommendations of the ARRIVE Guidelines for Reporting Animal Research. We used the C26 mouse cachectic model, which exhibits anorexia, weight loss, and muscle atrophy. Eight-week-old CD2F1 male mice were purchased from Charles River Laboratories and were housed (4 per cage), at an ambient temperature of 22 °C and under regular light-dark cycles of 12 h with ad lib access to water and food (PicoLab 5053, LabDiet). Prior to tumor implantation, mice were assigned to groups matched for body weight, individually housed, and acclimated to the experimental conditions for

1 week. Tumor implantation was conducted when animals were 12-16 weeks old and had reached a stable stage in growth and weight gain. One million cxC26 or ncxC26 cells suspended in 200 µL of saline were implanted subcutaneously into the right flank of each mouse. The study was conducted over a period of two weeks. From day 0 to day 5 following tumor inoculation, all mice were provided with food ad libitum. Beginning on day 6, cxC26 mice and one group of ncxC26 mice were switched to an isocaloric feeding regimen, while a separate group of ncxC26 mice continued to receive food ad libitum. Body weight was recorded every other day post-implantation at a consistent time (between 11 am and 1 pm). Sacrifices were performed on day 12 post-injection. Mice were fasted for 7-8 hours before the tissue collection. The animals were then subjected to death by cervical dislocation. Blood was collected by cardiac puncture. Serum samples were obtained by centrifugation at 10,000 g for 10 minutes and stored at -80 °C until use. Tumors, tissues, and organs were harvested and weighed for mass data. For molecular analyses, tissues (liver, gastrocnemius, and soleus) were immediately dissected, clamped with a pre-chilled Wollenberger clamp, rapidly snap-frozen in liquid nitrogen, and stored at -80 °C until further use. All animal care and experimental procedures were approved all animal care and experimental procedures and Use Committees (IACUC) of Harvard Medical School and Harvard T.H. Chan School of Public Health.

METHOD DETAILS

Food intake measurement and isocaloric feeding

For food intake measurement, animals were singly housed on alpha pad bedding (6" × 10", ScottPharm solution) with virgin kraft crinkled paper strips as nesting material (Enviro-Dri™, ScottPharm solution) (See Figure S2A). Food intake was measured daily at a consistent time

(between 4:00 and 6:00 pm). Food pellets were weighed and put back on the cage lid. Any food debris on the bedding (See Figure S2A) was collected using a 2 mm stainless steel mesh sieve (Gilson Company, Inc.), weighed, recorded, and discarded. Food surplus was defined as the total of pellets remaining on the cage lid plus food debris collected from the bedding. Daily food intake was calculated as the difference between the amount of food provided and the food surplus over two consecutive days.

For the isocaloric feeding, the mice in all three groups were body weight-matched at baseline. A group of ncxC26 tumor-bearing mice was on ad lib as a control. From days 6 to 11 post-tumor injection, the cxC26 mice and another group of ncxC26 mice were fed an equal amount of food each day, matched to the intake of cxC26 mice measured previously (shown in Figure 1A). Food was checked daily between 4:00 and 6:00 pm, and fresh food was provided at 6:00 pm. Food debris from the bedding was collected daily using a 2 mm stainless steel mesh sieve (Gilson Company, Inc.), weighed, and discarded. An equivalent amount of food was then returned to the corresponding cage to ensure that both cxC26 and ncxC26 groups received identical total food quantities. Any mouse with more than 1g of uneaten food (about 5% of the total food intake of the isocaloric feeding) on day 12 would be excluded from the analysis.

Pair feeding

Food intake for the cxC26 mice was measured daily between 4:00 and 6:00 pm. Each day at 6:00 pm, the ncxC26 mice were provided with an amount of food equivalent to the average intake of the cxC26 group. For pair feeding with the cxC26nci mice, due to the heterogeneity within the cxC26-nci group, individual pair feeding was implemented. Specifically, each ncxC26 mouse was matched one-to-one with a cxC26nci mouse based on body weight, and received the same amount of food as its corresponding cxC26nci littermate.

Body composition assessment

Whole-body composition (fat and lean mass) was assessed for each animal on days 0 and 12 using an EchoMRI-100 (EchoMRI LLC). Mice were individually placed in a specialized plastic tube for mild conscious restraint and scanned for approximately 5 minutes. Following measurement, mice were returned to their home cages.

Metabolic cage analyses

Mice were individually housed at 22 °C on alpha pad bedding (6" × 10", ScottPharm solution) and subjected to indirect calorimetry between day 0 and day 12 after tumor inoculation under a 12 h light-dark cycle using the Promethion Metabolic Cage system (Sable Systems, USA). During this period, spontaneous activity, oxygen consumption (VO□), and carbon dioxide production (VCO□) were continuously measured to calculate energy expenditure (EE) and respiratory exchange ratio (RER).

Fecal energy determination

Feces produced 24 hours before the endpoint were collected and stored at -80 °C. The feces were dehydrated at 60 °C for 48 hours in an Eppendorf tube with the lid open. Then, the calorie content of the dry feces was determined by using Bomb Calorimetry (Parr Oxygen Bomb). Wet and dry fecal weights were recorded to calculate total fecal output (g/day) and fecal energy density (cal/g).

Grip strength

Grip strength was assessed using a Grip Strength Meter (Bioseb); mice were allowed to grasp a metal grid with all four limbs and were gently pulled backwards until release, with the peak force recorded.

Maximum exercise capacity test

Mice were acclimated to a motorized treadmill for three consecutive days (days 4-6) before the maximal exercise capacity test. Shocking grids with a frequency set at 2 Hz and an intensity of 1.22 mA were located at the end of the treadmill to encourage the mice to run at their maximum capacity. The treadmill was set at a 10° incline. The exercise test was performed at the end of day 12. Mice ran at 6 m/min for 2 minutes, 10 m/min for the next 8 minutes, and then the speed was increased by 2 m/min every 5 minutes until exhaustion. Exhaustion was defined as the inability to remain on the treadmill for more than 5 seconds, spending more than 50% of the time on the shock grid, or remaining on the grid for more than 2 seconds on more than three occasions.

RNA extraction and RT-qPCR

Total RNA was extracted using the Trizol reagent (Invitrogen, #15596026) from the 20-30 mg of gastrocnemius, following the manufacturer's protocol. RNA concentration was determined using NanoDrop One (Thermofisher Scientific). One microgram of purified RNA was converted to cDNA using the iScript Reverse Transcription Supermix for RT-qPCR (Bio-Rad, #1708840). The diluted cDNA was used for RT-qPCR using SsoAdvanced Universal SYBR Green Supermix (Bio-Rad, #1725270) with the CFX384 Real-Time PCR detection System (Bio-Rad). The following primer sequences were used to determine the Atrogin-1 and MuRF1 mRNA expression. Cyclophilin was used as a housekeeping gene for normalization.

Measurement of glycogen in tissues

Frozen tissues were then ground under cryogenic condition using a CryoMill (Retsch). For glycogen quantification, 10 – 20 µg of ground tissue were used in the Glycogen-Glo assay kit (Promega, #J5051), following the manufacturer's instructions.

Serum metabolomics

Serum metabolites were extracted using extraction buffer (acetonitrile: methanol: water, 4: 4: 2, *v: v: v*) at a volume-to-volume ratio of 1:20 (μL to μL), followed immediately by vortexing for 10 seconds. The mixture was then incubated at 4 °C for 10 min before centrifugation at 16,000 g at 4 °C for 10 min. The supernatant was transferred to an LC-MS vial and analyzed on the LC-MS. A pooled quality control (QC) sample was prepared by mixing 20 μL from each experimental sample.

Metabolite extracts were analyzed using a quadrupole-orbitrap mass spectrometer coupled with hydrophilic interaction chromatography (HILIC). Chromatographic separation was achieved on an XBridge BEH Amide XP Column (2.5 μm, 2.1 mm × 150 mm) with a guard column (2.5 μm, 2.1 mm × 5 mm) (Waters, Milford, MA). For the gradient, mobile phase A was water: acetonitrile 95:5, and mobile phase B was water: acetonitrile 20:80, both phases containing 10 mM ammonium acetate and 10 mM ammonium hydroxide. The linear elution gradient was: 0 ~ 3 min, 100% B; 3.2 ~ 6.2 min, 90% B; 6.5. ~ 10.5 min, 80% B; 10.7 ~ 13.5 min, 70% B; 13.7 ~ 16 min, 45% B; and 16.5 ~ 22 min, 100% B, with a flow rate of 0.3 mL/ min. The autosampler was at 4˚C. The column temperature was at 30˚C. The injection volume was 5 μL. Needle wash was applied between samples using acetonitrile: methanol: water at 4: 4: 2 (*v: v: v*). For mass spectrometry, a Q Exactive HF (Thermo Fisher Scientific, San Jose, CA) mass spectrometer was used. For MS1 acquisition, the MS scanned from 70 to 1000 m/z with switching polarity at a resolution of 120,000 for all experimental samples. The relevant parameters were: sheath gas, 40; auxiliary gas, 10; sweep gas, 2; spray voltage, 3.5 kV; capillary temperature, 300 °C; S-lens, 45. The resolution was set at 120,000 (at m/z 200). Maximum injection time (max IT) was set at 500 ms, and automatic gain control (AGC) was set at 3×10^6.

MS1 raw data files were converted into mzxML using msconvert and imported to EI-Maven (Elucidata, Cambridge, MA) for targeted metabolomics. Metabolites were identified using an in-house library based on accurate mass and retention time.

QUANTIFICATION AND STATISTICAL ANALYSIS

Isocaloric-fed mice that accumulated more than 1 g of uneaten food were excluded from the study. Statistical analyses for the data presented in Figures 1–4 were performed using GraphPad Prism 10, with the assumption that data were normally distributed and had equal standard deviations. Serum metabolomics data (Figure 5) were analyzed in RStudio, where mass spectrometry readings were log-transformed to achieve normality and equal variance among the three groups. Comparisons between three groups were conducted using one-way ANOVA, followed by Tukey's post hoc test. Quantitative results are expressed as mean ± standard deviation (s.d.). Metabolites with adjusted p-values less than 0.05 were considered significant. For all analyses, a p-value < 0.05 was considered statistically significant (*$p < 0.05$, **$p < 0.01$, ***$p < 0.001$, ****$p < 0.0001$).

Supplemental information

Document S1. Figures S1-S6 and Table S1.

Reference

1. Fearon, K., Strasser, F., Anker, S.D., Bosaeus, I., Bruera, E., Fainsinger, R.L., Jatoi, A., Loprinzi, C., MacDonald, N., Mantovani, G., et al. (2011). Definition and classification of cancer cachexia: an international consensus. The Lancet Oncology *12*, 489–495. https://doi.org/10.1016/S1470-2045(10)70218-7.

2. Peixoto Da Silva, S., Santos, J.M.O., Costa E Silva, M.P., Gil Da Costa, R.M., and Medeiros, R. (2020). Cancer cachexia and its pathophysiology: links with sarcopenia, anorexia and asthenia. J cachexia sarcopenia muscle *11*, 619–635. https://doi.org/10.1002/jcsm.12528.

3. Fearon, K., Arends, J., and Baracos, V. (2013). Understanding the mechanisms and treatment options in cancer cachexia. Nat Rev Clin Oncol *10*, 90–99. https://doi.org/10.1038/nrclinonc.2012.209.

4. Kwon, Y.-Y., and Hui, S. (2024). IL-6 promotes tumor growth through immune evasion but is dispensable for cachexia. EMBO Rep *25*, 2592–2609. https://doi.org/10.1038/s44319-024-00144-3.

5. Weiss, E.P., Jordan, R.C., Frese, E.M., Albert, S.G., and Villareal, D.T. (2017). Effects of Weight Loss on Lean Mass, Strength, Bone, and Aerobic Capacity. Medicine & Science in Sports & Exercise *49*, 206–217. https://doi.org/10.1249/MSS.0000000000001074.

6. He, Y., Yang, W., Huang, L., Mever, M.A., Ramautar, R., Harms, A., Rijksen, Y., Brandt, R.M.C., Barnhoorn, S., Smit, K., et al. (2024). Metabolomic analysis of dietary‐restriction‐induced attenuation of sarcopenia in prematurely aging DNA repair‐deficient mice. J cachexia sarcopenia muscle *15*, 868–882. https://doi.org/10.1002/jcsm.13433.

7. Most, J., and Redman, L.M. (2020). Impact of calorie restriction on energy metabolism in humans. Experimental Gerontology *133*, 110875. https://doi.org/10.1016/j.exger.2020.110875.

8. Belury (2010). Cardiac alterations in cancer-induced cachexia in mice. Int J Oncol *37*. https://doi.org/10.3892/ijo_00000683.

9. Tsoli, M., Moore, M., Burg, D., Painter, A., Taylor, R., Lockie, S.H., Turner, N., Warren, A., Cooney, G., Oldfield, B., et al. (2012). Activation of Thermogenesis in Brown Adipose Tissue and Dysregulated Lipid Metabolism Associated with Cancer Cachexia in Mice. Cancer Research *72*, 4372–4382. https://doi.org/10.1158/0008-5472.CAN-11-3536.

10. Kliewer, K.L., Ke, J.-Y., Tian, M., Cole, R.M., Andridge, R.R., and Belury, M.A. (2015). Adipose tissue lipolysis and energy metabolism in early cancer cachexia in mice. Cancer Biology & Therapy *16*, 886–897. https://doi.org/10.4161/15384047.2014.987075.

11. Reddel, C.J., Allen, J.D., Ehteda, A., Taylor, R., Chen, V.M.Y., Curnow, J.L., Kritharides, L., and Robertson, G. (2017). Increased thrombin generation in a mouse model of cancer cachexia is partially interleukin‐6 dependent. Journal of Thrombosis and Haemostasis *15*, 477–486. https://doi.org/10.1111/jth.13612.

12. Chen, X., Wu, Q., Gong, W., Ju, S., Fan, J., Gao, X., Liu, X., Lei, X., Liu, S., Ming, X., et al. (2024). GRP75 triggers white adipose tissue browning to promote cancer-associated cachexia. Sig Transduct Target Ther *9*, 253. https://doi.org/10.1038/s41392-024-01950-w.

13. Flint, T.R., Janowitz, T., Connell, C.M., Roberts, E.W., Denton, A.E., Coll, A.P., Jodrell, D.I., and Fearon, D.T. (2016). Tumor-Induced IL-6 Reprograms Host Metabolism to Suppress Anti-tumor Immunity. Cell Metabolism *24*, 672–684. https://doi.org/10.1016/j.cmet.2016.10.010.

14. Sudo, Y., Otsuka, H., Miyakawa, R., Goto, A., Kashiwase, Y., Terawaki, K., Miyano, K., Hirao, Y., Taki, K., Tagawa, R., et al. (2018). Differential Metabolic Responses to Adipose Atrophy Associated with Cancer Cachexia and Caloric Restriction in Rats and the Effect of Rikkunshito in Cancer Cachexia. IJMS *19*, 3852. https://doi.org/10.3390/ijms19123852.

15. Bonetto, A., Rupert, J.E., Barreto, R., and Zimmers, T.A. (2016). The Colon-26 Carcinoma Tumor-bearing Mouse as a Model for the Study of Cancer Cachexia. JoVE, 54893. https://doi.org/10.3791/54893.

16. Flint, T.R., Janowitz, T., Connell, C.M., Roberts, E.W., Denton, A.E., Coll, A.P., Jodrell, D.I., and Fearon, D.T. (2016). Tumor-Induced IL-6 Reprograms Host Metabolism to Suppress Anti-tumor Immunity. Cell Metabolism *24*, 672–684. https://doi.org/10.1016/j.cmet.2016.10.010.

17. Zhang, W., Sun, W., Gu, X., Miao, C., Feng, L., Shen, Q., Liu, X., and Zhang, X. (2022). GDF-15 in tumor-derived exosomes promotes muscle atrophy via Bcl-2/caspase-3 pathway. Cell Death Discov. *8*, 162. https://doi.org/10.1038/s41420-022-00972-z.

18. Rupp, H., Maisch, B., and Brilla, C.G. (1997). Schedule-induced psychological stress and molecular structures of cardiomyocytes. American Journal of Physiology-Regulatory, Integrative and Comparative Physiology *272*, R776–R782. https://doi.org/10.1152/ajpregu.1997.272.3.R776.

19. Russell, J.C., Proctor, S.D., Kelly, S.E., and Brindley, D.N. (2008). Pair feeding-mediated changes in metabolism: stress response and pathophysiology in insulin-resistant, atherosclerosis-prone JCR:LA-cp rats. American Journal of Physiology-Endocrinology and Metabolism *294*, E1078–E1087. https://doi.org/10.1152/ajpendo.90257.2008.

20. Di Tano, M., Raucci, F., Vernieri, C., Caffa, I., Buono, R., Fanti, M., Brandhorst, S., Curigliano, G., Nencioni, A., De Braud, F., et al. (2020). Synergistic effect of fasting-mimicking diet and vitamin C against KRAS mutated cancers. Nat Commun *11*, 2332. https://doi.org/10.1038/s41467-020-16243-3.

21. Pomatto-Watson, L.C.D., Bodogai, M., Bosompra, O., Kato, J., Wong, S., Carpenter, M., Duregon, E., Chowdhury, D., Krishna, P., Ng, S., et al. (2021). Daily caloric restriction limits tumor growth more effectively than caloric cycling regardless of dietary composition. Nat Commun *12*, 6201. https://doi.org/10.1038/s41467-021-26431-4.

22. De Groot, S., Lugtenberg, R.T., Cohen, D., Welters, M.J.P., Ehsan, I., Vreeswijk, M.P.G., Smit, V.T.H.B.M., De Graaf, H., Heijns, J.B., Portielje, J.E.A., et al. (2020). Fasting mimicking diet as an adjunct to neoadjuvant chemotherapy for breast cancer in the multicentre randomized phase 2 DIRECT trial. Nat Commun *11*, 3083. https://doi.org/10.1038/s41467-020-16138-3.

23. Lee, C., and Longo, V.D. (2011). Fasting vs dietary restriction in cellular protection and cancer treatment: from model organisms to patients. Oncogene *30*, 3305–3316. https://doi.org/10.1038/onc.2011.91.

24. Kir, S., White, J.P., Kleiner, S., Kazak, L., Cohen, P., Baracos, V.E., and Spiegelman, B.M. (2014). Tumour-derived PTH-related protein triggers adipose tissue browning and cancer cachexia. Nature *513*, 100–104. https://doi.org/10.1038/nature13528.

25. Riner, A.N., Herremans, K.M., Vudatha, V., Han, S., Qu, X., Liu, J., Mukhopadhyay, N., Freudenberger, D.C., George, T.J., Judge, S.M., et al. (2024). Heterogeneity of weight loss and transcriptomic signatures in pancreatic ductal adenocarcinoma. J cachexia sarcopenia muscle *15*, 149–158. https://doi.org/10.1002/jcsm.13390.

26. Bilgic, S.N., Domaniku, A., Toledo, B., Agca, S., Weber, B.Z.C., Arabaci, D.H., Ozornek, Z., Lause, P., Thissen, J.-P., Loumaye, A., et al. (2023). EDA2R–NIK signalling promotes muscle atrophy linked to cancer cachexia. Nature *617*, 827–834. https://doi.org/10.1038/s41586-023-06047-y.

27. Liu, X., Li, S., Cui, Q., Guo, B., Ding, W., Liu, J., Quan, L., Li, X., Xie, P., Jin, L., et al. (2024). Activation of GPR81 by lactate drives tumour-induced cachexia. Nat Metab. https://doi.org/10.1038/s42255-024-01011-0.

28. Kilgour, R.D., Vigano, A., Trutschnigg, B., Hornby, L., Lucar, E., Bacon, S.L., and Morais, J.A. (2010). Cancer‐related fatigue: the impact of skeletal muscle mass and strength in patients with advanced cancer. J cachexia sarcopenia muscle *1*, 177–185. https://doi.org/10.1007/s13539-010-0016-0.

29. Romero, S.A.D., Jones, L., Bauml, J.M., Li, Q.S., Cohen, R.B., and Mao, J.J. (2018). The association between fatigue and pain symptoms and decreased physical activity after cancer. Support Care Cancer *26*, 3423–3430. https://doi.org/10.1007/s00520-018-4203-4.

30. Dougherty, J.P., Springer, D.A., Cullen, M.J., and Gershengorn, M.C. (2019). Evaluation of the effects of chemotherapy-induced fatigue and pharmacological interventions in multiple mouse behavioral assays. Behavioural Brain Research *360*, 255–261. https://doi.org/10.1016/j.bbr.2018.12.011.

31. Dougherty, J.P., Springer, D.A., and Gershengorn, M.C. (2016). The Treadmill Fatigue Test: A Simple, High-throughput Assay of Fatigue-like Behavior for the Mouse. JoVE, 54052. https://doi.org/10.3791/54052-v.

32. Lu, S., Li, Y., Shen, Q., Zhang, W., Gu, X., Ma, M., Li, Y., Zhang, L., Liu, X., and Zhang, X. (2021). Carnosol and its analogues attenuate muscle atrophy and fat lipolysis induced by cancer cachexia. Journal of Cachexia, Sarcopenia and Muscle *12*, 779–795. https://doi.org/10.1002/jcsm.12710.

33. Dolly, A., Pötgens, S.A., Thibaut, M.M., Neyrinck, A.M., de Castro, G.S., Galbert, C., Lefevre, C., Wyart, E., Gomes, S.P., Gonçalves, D.C., et al. (2023). Impairment of aryl hydrocarbon receptor signalling promotes hepatic disorders in cancer cachexia. J Cachexia Sarcopenia Muscle *14*, 1569–1582. https://doi.org/10.1002/jcsm.13246.

34. Chaouki, G., Parry, L., Vituret, C., Jousse, C., Leremboure, M., Bourgne, C., Mosoni, L., Delorme, Y., Djelloul-Mazouz, M., Hermet, J., et al. (2025). Pre-cachectic changes in amino

acid homeostasis precede activation of eIF2α signaling in the liver at the onset of C26 cancer-induced cachexia. iScience *28*. https://doi.org/10.1016/j.isci.2025.112030.

35. Dwarkasing, J.T., Boekschoten, M.V., Argilès, J.M., van Dijk, M., Busquets, S., Penna, F., Toledo, M., Laviano, A., Witkamp, R.F., and van Norren, K. (2015). Differences in food intake of tumour-bearing cachectic mice are associated with hypothalamic serotonin signalling. J Cachexia Sarcopenia Muscle *6*, 84–94. https://doi.org/10.1002/jcsm.12008.

36. Rohm, M., Schäfer, M., Laurent, V., Üstünel, B.E., Niopek, K., Algire, C., Hautzinger, O., Sijmonsma, T.P., Zota, A., Medrikova, D., et al. (2016). An AMP-activated protein kinase–stabilizing peptide ameliorates adipose tissue wasting in cancer cachexia in mice. Nat Med *22*, 1120–1130. https://doi.org/10.1038/nm.4171.

37. Khamoui, A.V., Tokmina-Roszyk, D., Rossiter, H.B., Fields, G.B., and Visavadiya, N.P. (2020). Hepatic proteome analysis reveals altered mitochondrial metabolism and suppressed acyl-CoA synthetase-1 in colon-26 tumor-induced cachexia. Physiol Genomics *52*, 203–216. https://doi.org/10.1152/physiolgenomics.00124.2019.

38. Pranzini, E., Muccillo, L., Nesi, I., Santi, A., Mancini, C., Lori, G., Genovese, M., Lottini, T., Comito, G., Caselli, A., et al. (2024). Limiting serine availability during tumor progression promotes muscle wasting in cancer cachexia. Cell Death Discov. *10*, 510. https://doi.org/10.1038/s41420-024-02271-1.

39. Lin, K., Wei, L., Wang, R., Li, L., Song, S., Wang, F., He, M., Pu, W., Wang, J., Wazir, J., et al. (2024). Disrupted methionine cycle triggers muscle atrophy in cancer cachexia through epigenetic regulation of REDD1. Cell Metabolism, S1550413124004133. https://doi.org/10.1016/j.cmet.2024.10.017.

40. Tisdale, M.J. (1999). Wasting in Cancer. The Journal of Nutrition *129*, 243S-246S. https://doi.org/10.1093/jn/129.1.243S.

41. Petruzzelli, M., Schweiger, M., Schreiber, R., Campos-Olivas, R., Tsoli, M., Allen, J., Swarbrick, M., Rose-John, S., Rincon, M., Robertson, G., et al. (2014). A Switch from White to Brown Fat Increases Energy Expenditure in Cancer-Associated Cachexia. Cell Metabolism *20*, 433–447. https://doi.org/10.1016/j.cmet.2014.06.011.

42. Škop, V., Guo, J., Liu, N., Xiao, C., Hall, K.D., Gavrilova, O., and Reitman, M.L. (2023). The metabolic cost of physical activity in mice using a physiology-based model of energy expenditure. Molecular Metabolism *71*, 101699. https://doi.org/10.1016/j.molmet.2023.101699.

43. Queiroz, A.L., Dantas, E., Ramsamooj, S., Murthy, A., Ahmed, M., Zunica, E.R.M., Liang, R.J., Murphy, J., Holman, C.D., Bare, C.J., et al. (2022). Blocking ActRIIB and restoring appetite reverses cachexia and improves survival in mice with lung cancer. Nat Commun *13*, 4633. https://doi.org/10.1038/s41467-022-32135-0.

44. Kolnes, K.J., Nilsen, E.T.F., Brufladt, S., Meadows, A.M., Jeppesen, P.B., Skattebo, Ø., Johansen, E.I., Birk, J.B., Højlund, K., Hingst, J., et al. (2025). Effects of seven days' fasting

on physical performance and metabolic adaptation during exercise in humans. Nat Commun *16*, 122. https://doi.org/10.1038/s41467-024-55418-0.

45. Racette, S.B., Rochon, J., Uhrich, M.L., Villareal, D.T., Das, S.K., Fontana, L., Bhapkar, M., Martin, C.K., Redman, L.M., Fuss, P.J., et al. (2017). Effects of Two Years of Calorie Restriction on Aerobic Capacity and Muscle Strength. Medicine & Science in Sports & Exercise *49*, 2240–2249. https://doi.org/10.1249/MSS.0000000000001353.

46. Brown, J.L., Rosa-Caldwell, M.E., Lee, D.E., Blackwell, T.A., Brown, L.A., Perry, R.A., Haynie, W.S., Hardee, J.P., Carson, J.A., Wiggs, M.P., et al. (2017). Mitochondrial degeneration precedes the development of muscle atrophy in progression of cancer cachexia in tumour-bearing mice: Mitochondrial degeneration precedes cancer cachexia. Journal of Cachexia, Sarcopenia and Muscle *8*, 926–938. https://doi.org/10.1002/jcsm.12232.

47. Zhu, X.A., Starosta, S., Ferrer, M., Hou, J., Chevy, Q., Lucantonio, F., Muñoz-Castañeda, R., Zhang, F., Zang, K., Zhao, X., et al. (2025). A neuroimmune circuit mediates cancer cachexia-associated apathy. Science *388*, eadm8857. https://doi.org/10.1126/science.adm8857.

48. Temel, J.S., Abernethy, A.P., Currow, D.C., Friend, J., Duus, E.M., Yan, Y., and Fearon, K.C. (2016). Anamorelin in patients with non-small-cell lung cancer and cachexia (ROMANA 1 and ROMANA 2): results from two randomised, double-blind, phase 3 trials. The Lancet Oncology *17*, 519–531. https://doi.org/10.1016/S1470-2045(15)00558-6.

49. Katakami, N., Uchino, J., Yokoyama, T., Naito, T., Kondo, M., Yamada, K., Kitajima, H., Yoshimori, K., Sato, K., Saito, H., et al. (2018). Anamorelin (ONO‐7643) for the treatment of patients with non−small cell lung cancer and cachexia: Results from a randomized, double‐blind, placebo‐controlled, multicenter study of Japanese patients (ONO‐7643‐04). Cancer *124*, 606–616. https://doi.org/10.1002/cncr.31128.

50. Suriben, R., Chen, M., Higbee, J., Oeffinger, J., Ventura, R., Li, B., Mondal, K., Gao, Z., Ayupova, D., Taskar, P., et al. (2020). Antibody-mediated inhibition of GDF15–GFRAL activity reverses cancer cachexia in mice. Nat Med *26*, 1264–1270. https://doi.org/10.1038/s41591-020-0945-x.

51. Kim-Muller, J.Y., Song, L., LaCarubba Paulhus, B., Pashos, E., Li, X., Rinaldi, A., Joaquim, S., Stansfield, J.C., Zhang, J., Robertson, A., et al. (2023). GDF15 neutralization restores muscle function and physical performance in a mouse model of cancer cachexia. Cell Reports *42*, 111947. https://doi.org/10.1016/j.celrep.2022.111947.

52. Groarke, J.D., Crawford, J., Collins, S.M., Lubaczewski, S., Roeland, E.J., Naito, T., Hendifar, A.E., Fallon, M., Takayama, K., Asmis, T., et al. (2024). Ponsegromab for the Treatment of Cancer Cachexia. N Engl J Med, NEJMoa2409515. https://doi.org/10.1056/NEJMoa2409515.

53. Rohm, M., Zeigerer, A., Machado, J., and Herzig, S. (2019). Energy metabolism in cachexia. EMBO reports *20*, e47258. https://doi.org/10.15252/embr.201847258.

54. Perez, M.M., Newcomer, A.D., Moertel, C.G., Go, V.L., and Dimagno, E.P. (1983). Assessment of weight loss, food intake, fat metabolism, malabsorption, and treatment of pancreatic insufficiency in pancreatic cancer. Cancer *52*, 346–352. https://doi.org/10.1002/1097-0142(19830715)52:2%253C346::aid-cncr2820520228%253E3.0.co;2-z.

55. Ziemons, J., Smidt, M.L., Damink, S.O., and Rensen, S.S. (2021). Gut microbiota and metabolic aspects of cancer cachexia. Best Practice & Research Clinical Endocrinology & Metabolism *35*, 101508. https://doi.org/10.1016/j.beem.2021.101508.

56. Kaltenecker, D., Fisker Schmidt, S., Weber, P., Loft, A., Morigny, P., Machado, J., Geppert, J., Saul, K.B., Benedikt, P., Molocea, C.-E., et al. (2025). Functional liver genomics identifies hepatokines promoting wasting in cancer cachexia. Cell, S009286742500741X. https://doi.org/10.1016/j.cell.2025.06.039.

57. Brattain, M.G., Strobel-Stevens, J., Fine, D., Webb, M., and Sarrif, A.M. (1980). Establishment of mouse colonic carcinoma cell lines with different metastatic properties. Cancer Res *40*, 2142–2146.

58. Kandarian, S.C., Nosacka, R.L., Delitto, A.E., Judge, A.R., Judge, S.M., Ganey, J.D., Moreira, J.D., and Jackman, R.W. (2018). Tumour-derived leukaemia inhibitory factor is a major driver of cancer cachexia and morbidity in C26 tumour-bearing mice. J Cachexia Sarcopenia Muscle *9*, 1109–1120. https://doi.org/10.1002/jcsm.12346.

Figure 1

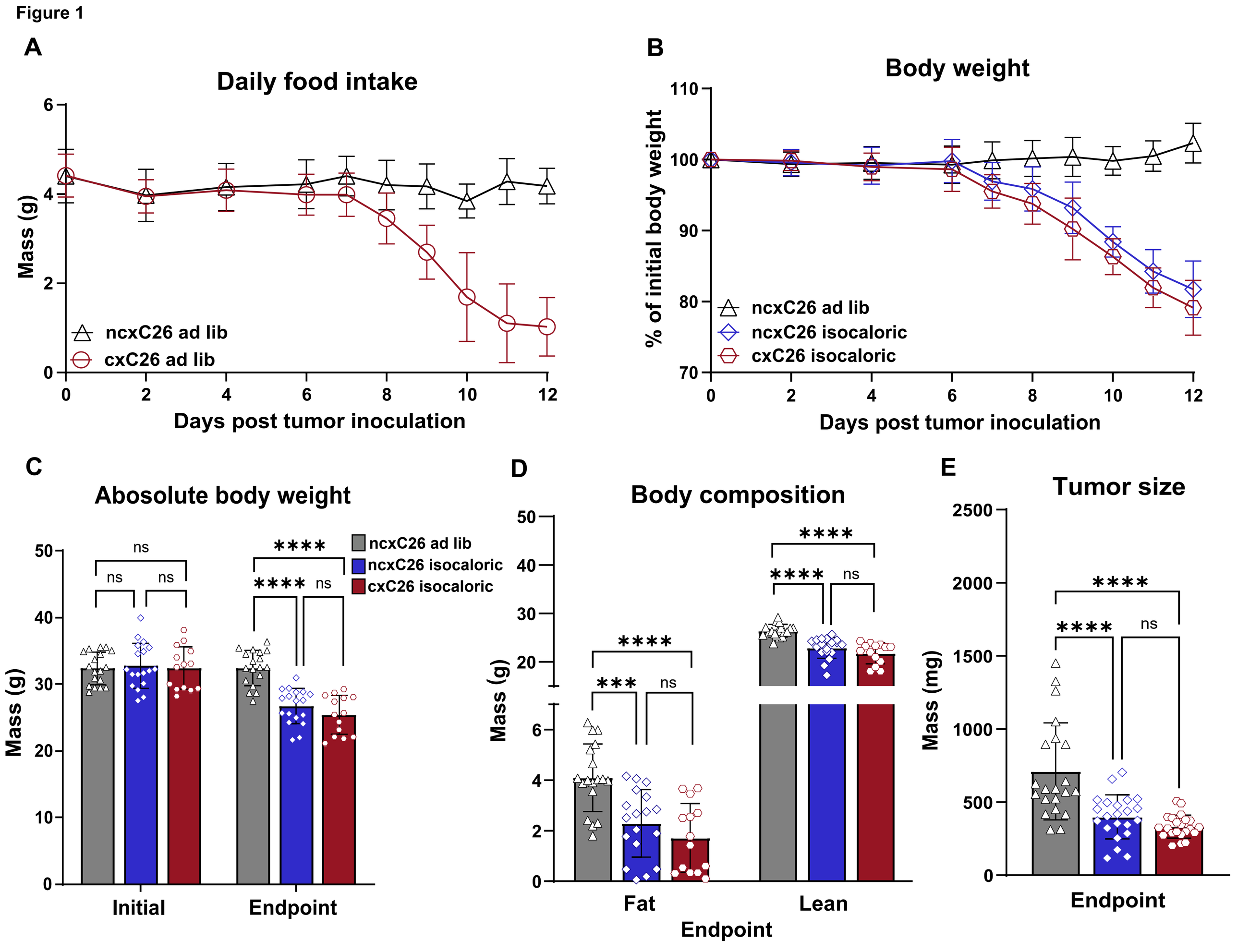
A
Daily food intake
Mass (g)
Days post tumor inoculation
ncxC26 ad lib
cxC26 ad lib
B
Body weight
% of initial body weight
Days post tumor inoculation
ncxC26 ad lib
ncxC26 isocaloric
cxC26 isocaloric
C
Abosolute body weight
Mass (g)
ns
ns
ns
****
****
ns
ncxC26 ad lib
ncxC26 isocaloric
cxC26 isocaloric
Initial
Endpoint
D
Body composition
Mass (g)
****
***
ns
****
****
ns
Fat
Lean
Endpoint
E
Tumor size
Mass (mg)
****
****
ns
Endpoint

Figure 2

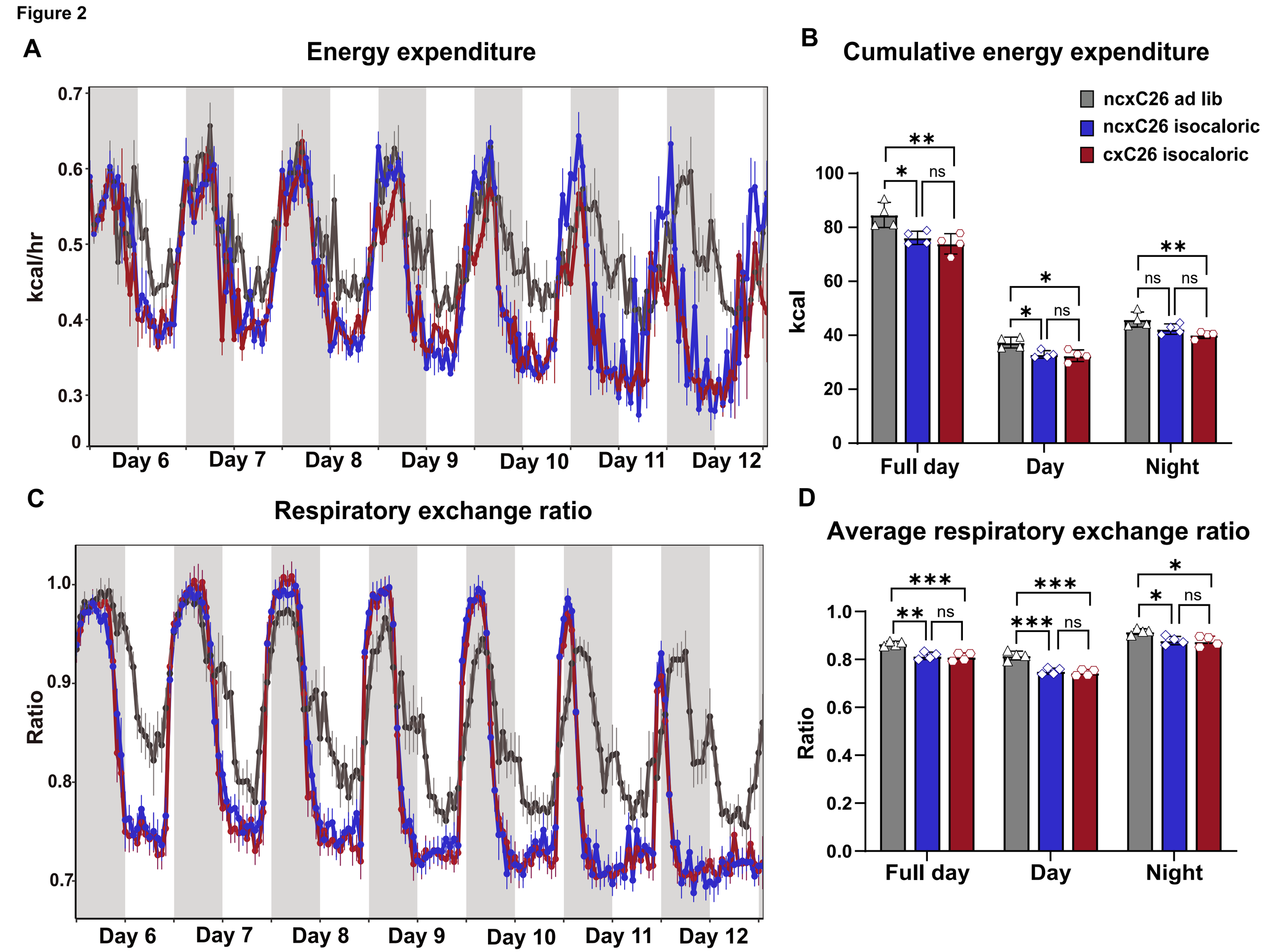
A
Energy expenditure
kcal/hr
0.7
0.6
0.5
0.4
0.3
0
Day 6
Day 7
Day 8
Day 9
Day 10
Day 11
Day 12
B
Cumulative energy expenditure
ncxC26 ad lib
ncxC26 isocaloric
cxC26 isocaloric
kcal
100
80
60
40
20
0
**
*
ns
*
*
ns
**
ns
ns
Full day
Day
Night
C
Respiratory exchange ratio
Ratio
1.0
0.9
0.8
0.7
Day 6
Day 7
Day 8
Day 9
Day 10
Day 11
Day 12
D
Average respiratory exchange ratio
Ratio
1.0
0.8
0.6
0.4
0.2
0.0
***
**
ns
***
***
ns
*
*
ns
Full day
Day
Night
E
Fecal production
Mass (g)
0.8
0.6
0.4
0.2
0.0
****
****
ns
F
Fecal energy density
Calorie density (kcal/g)
5
4
3
2
1
0
ns
ns
ns
G
Total fecal energy excretion
Calorie (kcal)
3
2
1
0
****
****
ns

Figure 3

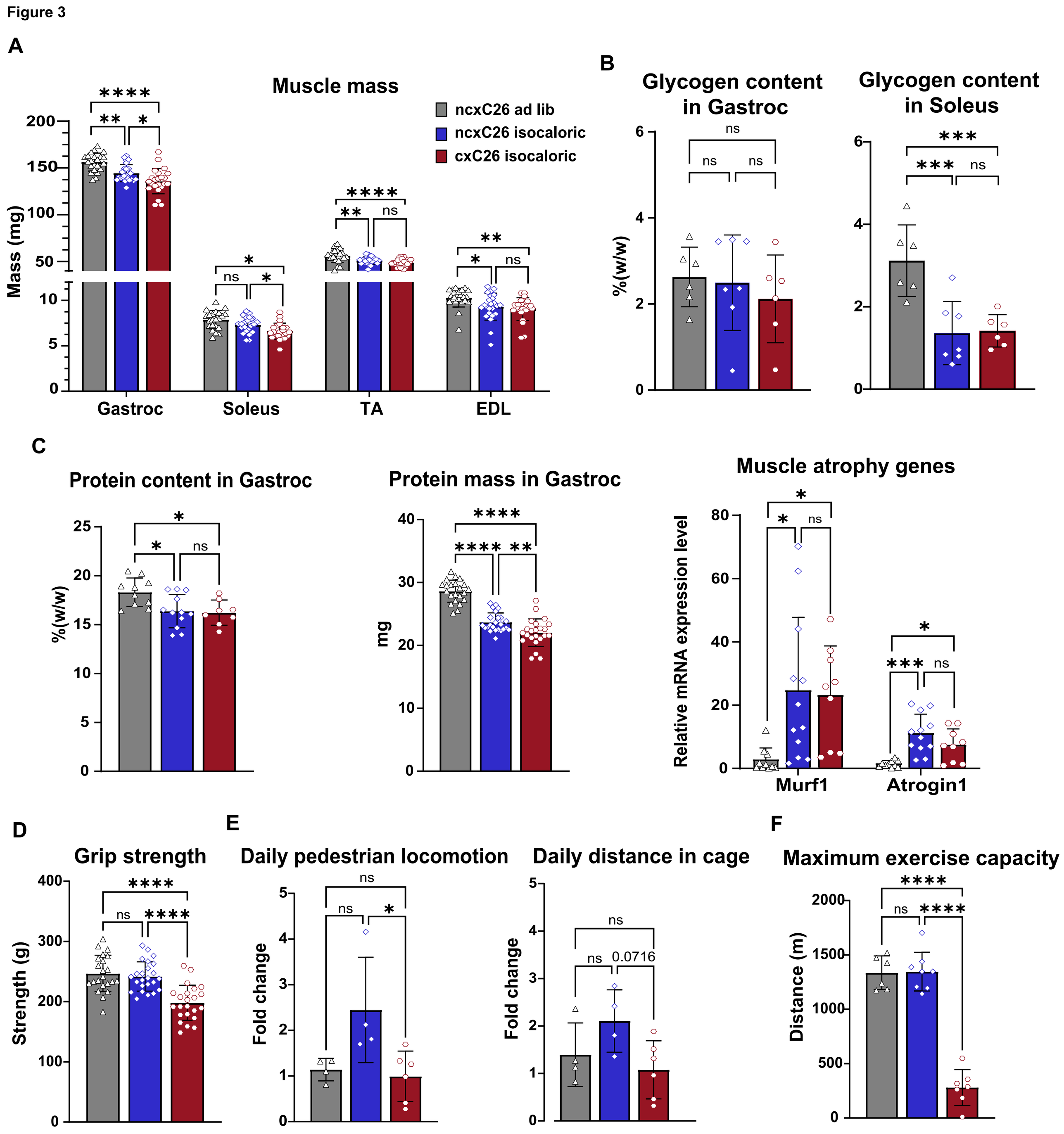
A
Muscle mass
ncxC26 ad lib
ncxC26 isocaloric
cxC26 isocaloric
Mass (mg)
Gastroc
Soleus
TA
EDL
B
Glycogen content in Gastroc
Glycogen content in Soleus
%(w/w)
C
Protein content in Gastroc
Protein mass in Gastroc
Muscle atrophy genes
Relative mRNA expression level
Murf1
Atrogin1
D
Grip strength
Strength (g)
E
Daily pedestrian locomotion
Fold change
Daily distance in cage
F
Maximum exercise capacity
Distance (m)

Figure 4

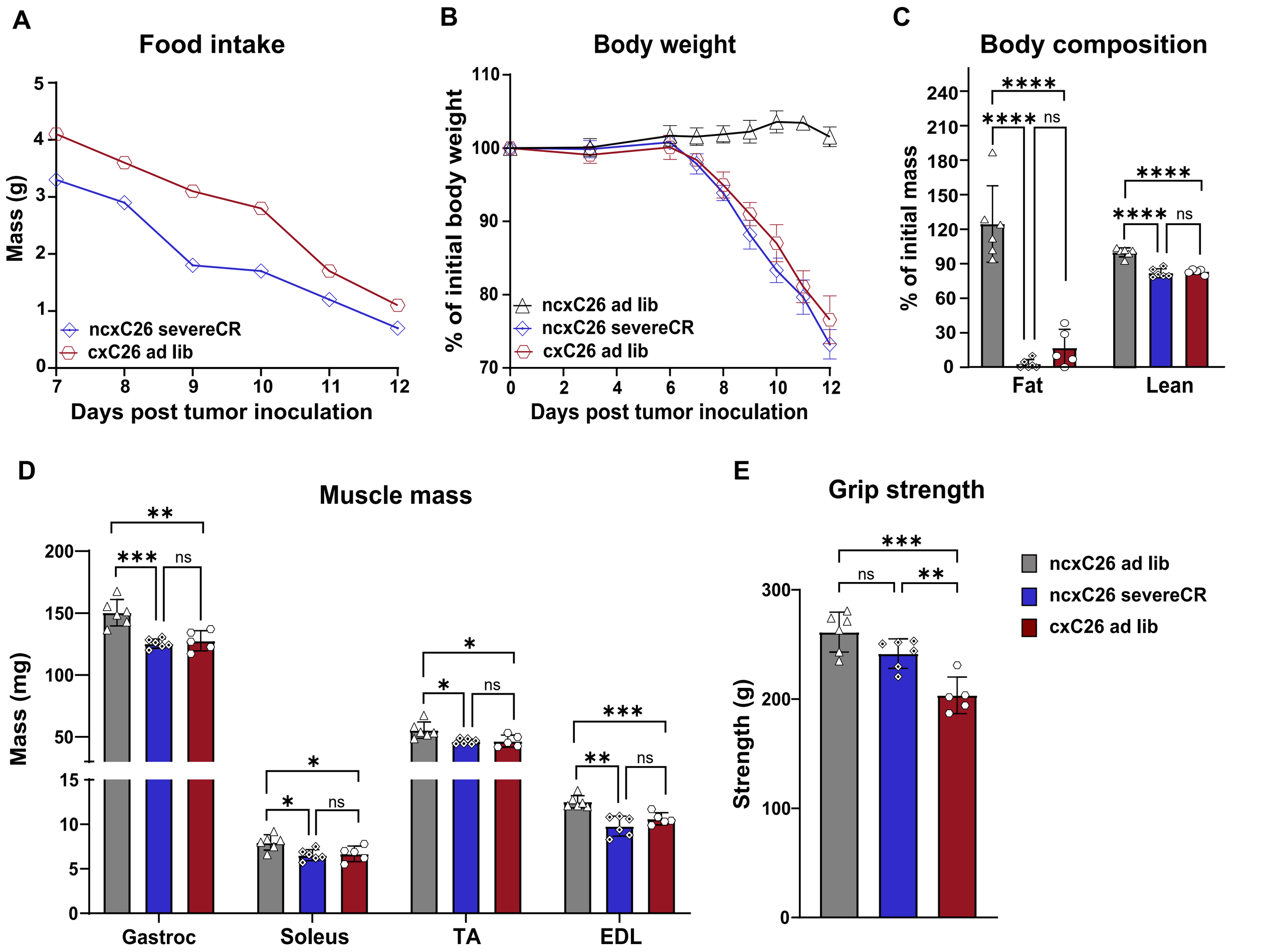
A
Food intake
Mass (g)
Days post tumor inoculation
ncxC26 severeCR
cxC26 ad lib
B
Body weight
% of initial body weight
Days post tumor inoculation
ncxC26 ad lib
ncxC26 severeCR
cxC26 ad lib
C
Body composition
% of initial mass
Fat
Lean
****
ns
D
Muscle mass
Mass (mg)
Gastroc
Soleus
TA
EDL
E
Grip strength
Strength (g)
ncxC26 ad lib
ncxC26 severeCR
cxC26 ad lib

Figure 5

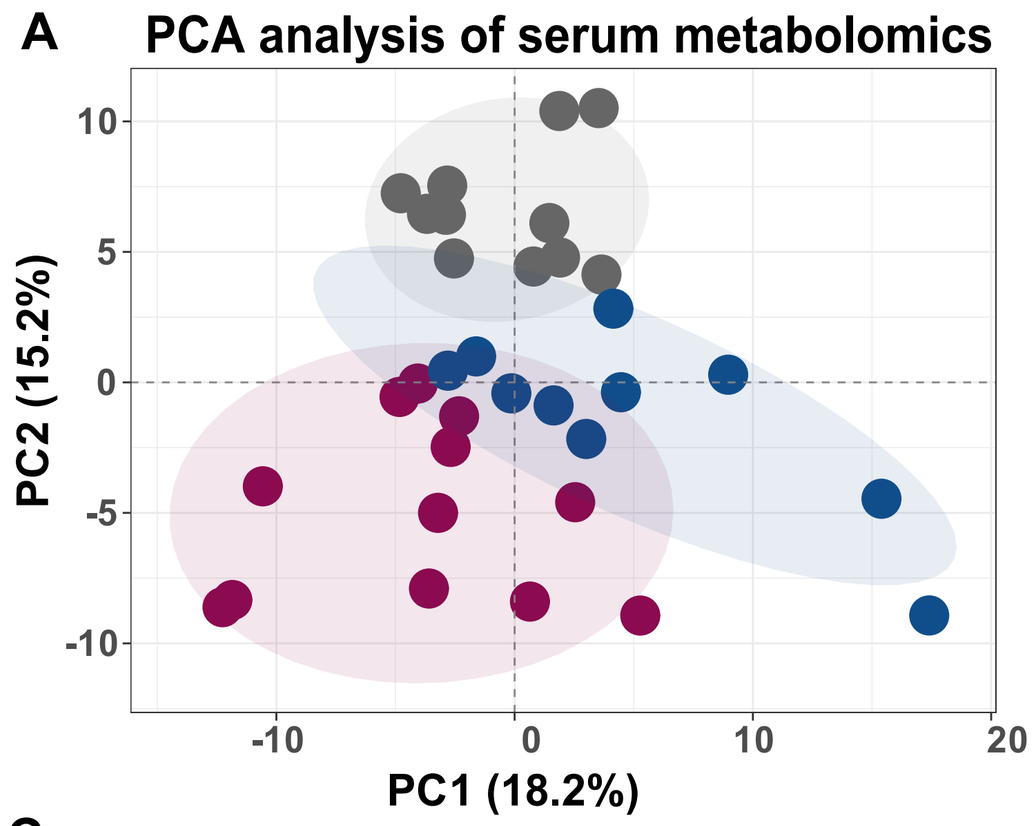
A
PCA analysis of serum metabolomics
PC2 (15.2%)
PC1 (18.2%)
10
5
0
-5
-10
-10
0
10
20

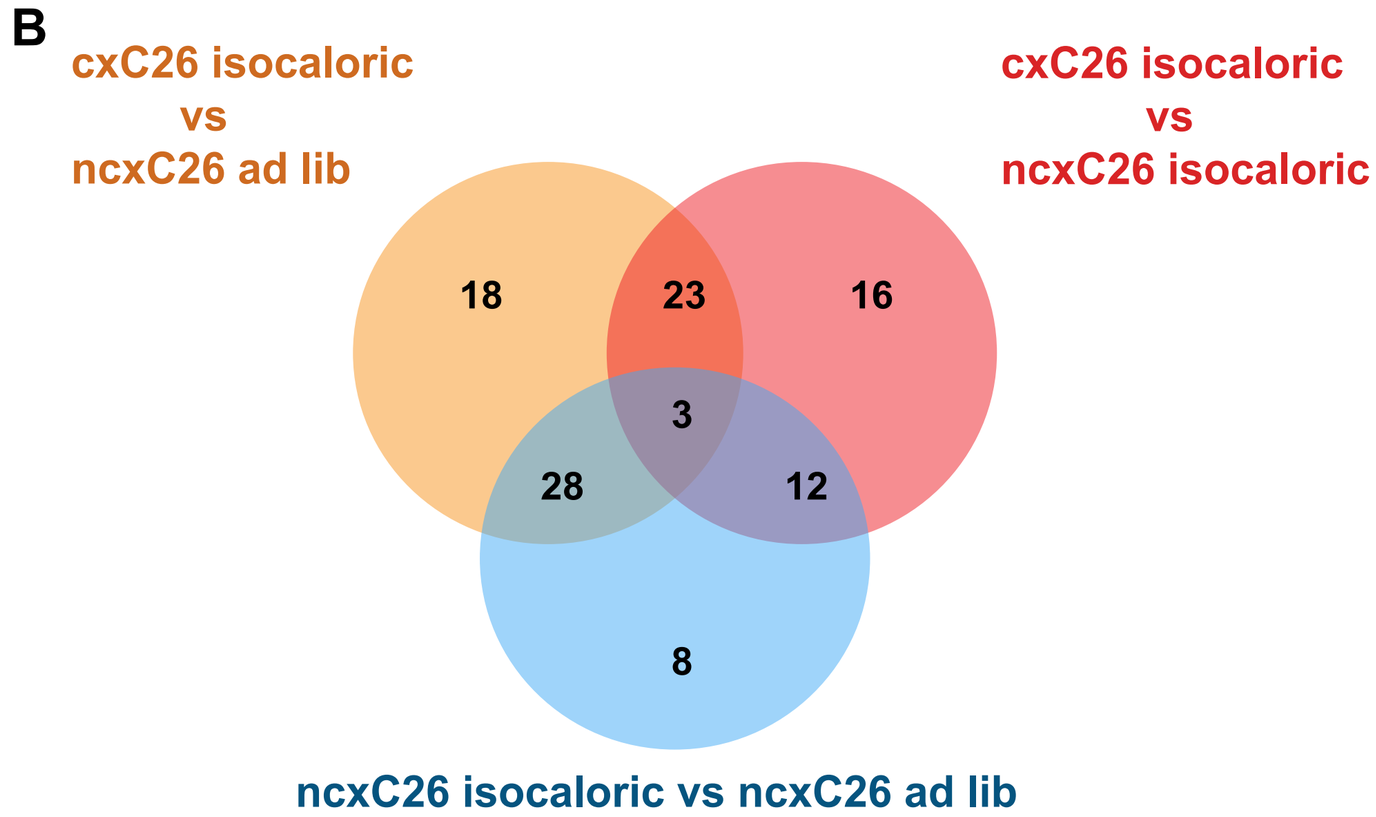
B
cxC26 isocaloric
vs
ncxC26 ad lib
cxC26 isocaloric
vs
ncxC26 isocaloric
ncxC26 isocaloric vs ncxC26 ad lib
18
23
16
3
28
12
8

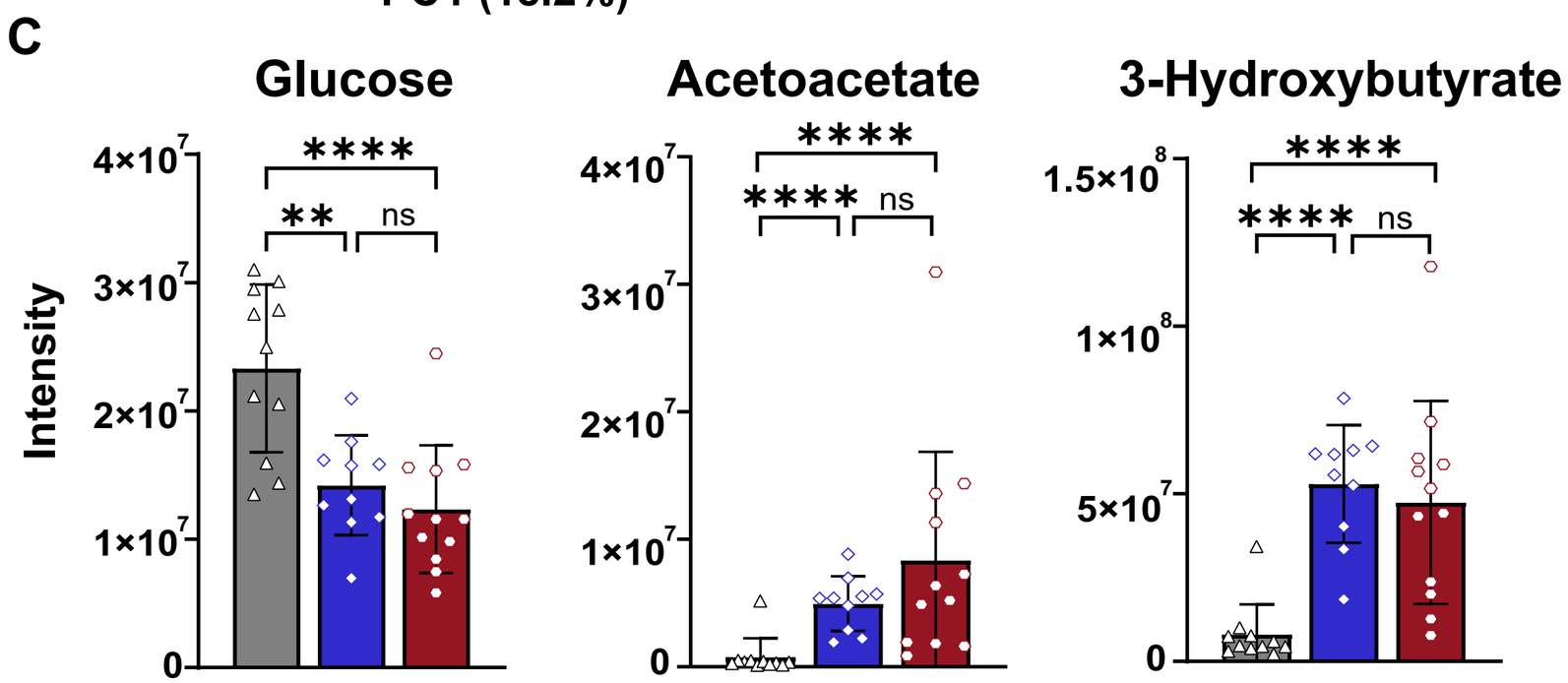
C
Glucose
Acetoacetate
3-Hydroxybutyrate
Intensity
4×10^7
3×10^7
2×10^7
1×10^7
0
1.5×10^8
1×10^8
5×10^7
****
**
ns

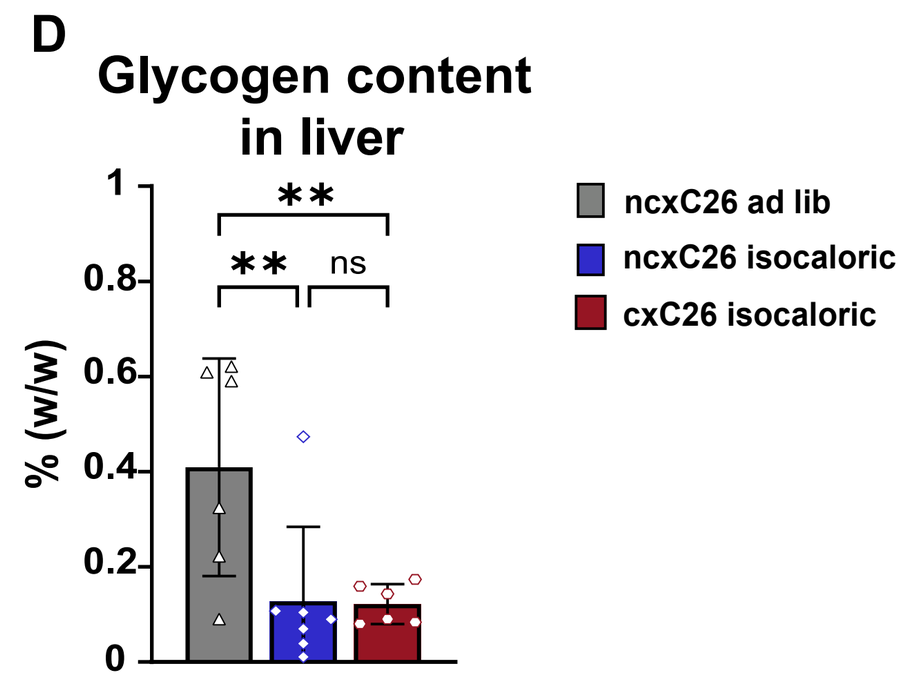
D
Glycogen content
in liver
% (w/w)
1
0.8
0.6
0.4
0.2
0
**
ns
ncxC26 ad lib
ncxC26 isocaloric
cxC26 isocaloric

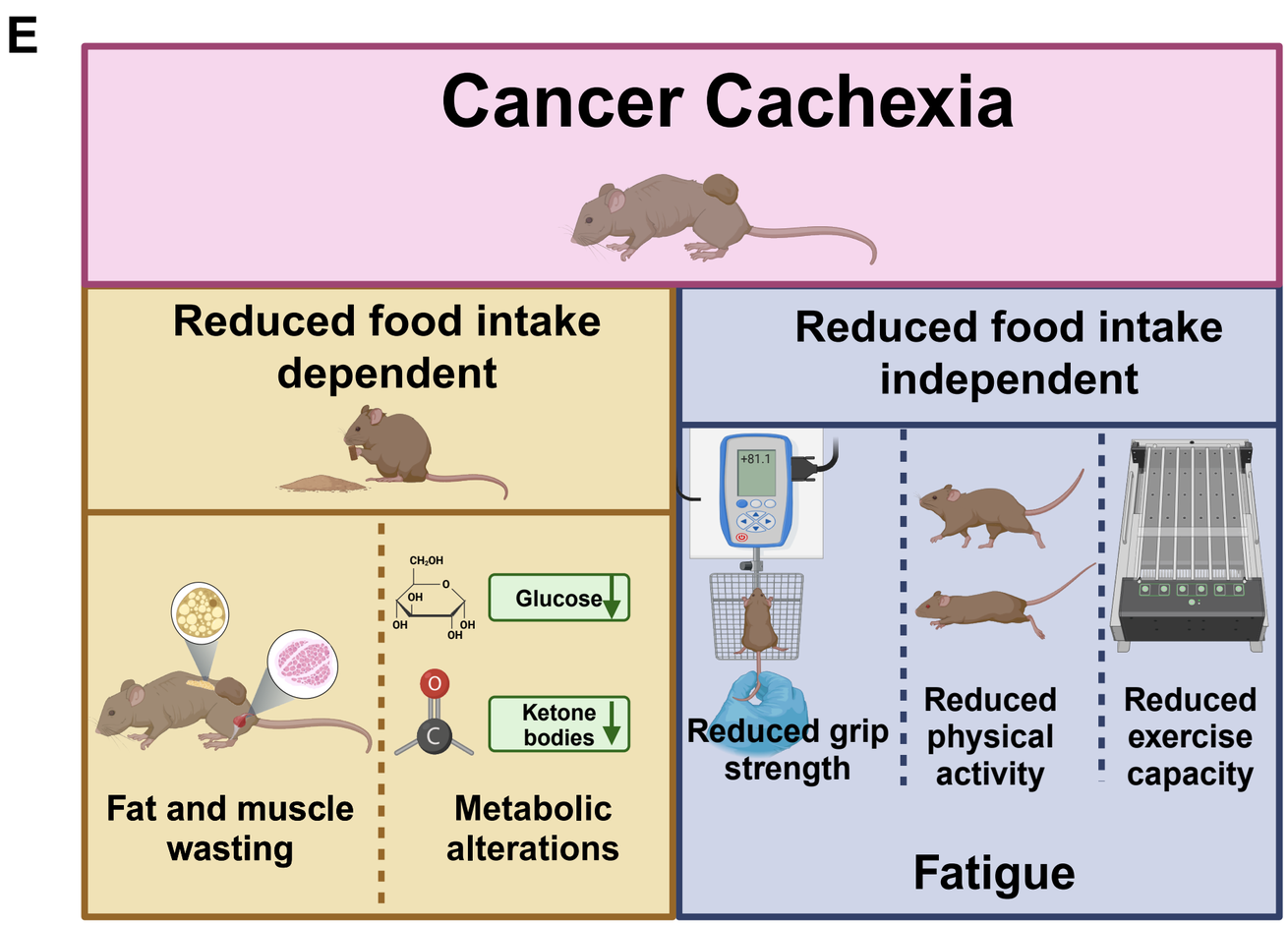
E
Cancer Cachexia
Reduced food intake
dependent
Reduced food intake
independent
Glucose
Ketone
bodies
Fat and muscle
wasting
Metabolic
alterations
Reduced grip
strength
Reduced
physical
activity
Reduced
exercise
capacity
Fatigue